9B.1

# TROPICAL STORM ERIN (2007): A POLARIMETRIC RADAR ANALYSIS OF EYEWALL AND RAINBAND CONVECTION DURING OVERLAND RE-INTENSIFICATION

Erica M. Griffin[1,2,3], Terry J. Schuur[1,2,3], Matthew R. Kumjian[1,2,3], and Donald R. MacGorman[2]

[1]Cooperative Institute for Mesoscale Meteorological Studies, University of Oklahoma
Norman, Oklahoma

[2]NOAA/OAR/National Severe Storms Laboratory
Norman, Oklahoma

[3]School of Meteorology, University of Oklahoma
Norman, Oklahoma

## 1. INTRODUCTION

Tropical Storm Erin formed over the Gulf of Mexico at approximately 0000 UTC on 15 August 2007 (Knabb 2008). As the system progressed toward the Texas coastline, it strengthened over the warm gulf water and reached tropical storm status by 1800 UTC 15 August (18 m $s^{-1}$ maximum sustained wind; Knabb 2008). Erin made landfall near Lamar, Texas as a tropical depression at approximately 1030 UTC 16 August (15.4 m $s^{-1}$ maximum sustained winds; Knabb 2008). After landfall, it continued northwestward into west Texas as a tropical depression before degenerating further and tracking northeast towards Oklahoma (OK) along the northwestern periphery of a strong midlevel ridge. Figure 1 illustrates the National Hurricane Center's best track for the system. While passing over west-central OK on 18-19 August, Erin's remnants unexpectedly re-intensified and developed an eye-like feature that was clearly discernable in WSR-88D radar imagery (Fig. 2). The eye was distinguishable between approximately 0800 UTC and 1300 UTC on 19 August, but rapidly dissipated after 1300 UTC. During this brief re-intensification period, the center of the low (as well as the newly-formed eye) traversed a dense region of surface and remote sensing observation networks that provided abundant data of high spatial and temporal resolution. In this study, we examine data from the polarimetric prototype of the WSR-88D KOUN radar in an attempt to compare the structure of the convection to that of tropical storms that have been observed over open water, as well as to better understand the possible role of the eyewall convection in the re-intensification process. Electrical characteristics of the system are also presented using total lightning data from the Oklahoma Lightning Mapping Array (OK-LMA) and ground-flash data from the National Lightning Detection Network (NLDN).

Corresponding author address: Erica M. Griffin
University of Oklahoma/School of Meteorology
National Weather Center
120 David L. Boren Blvd., Norman, OK, 73072
E-mail: Erica.m.griffin-1@ou.edu

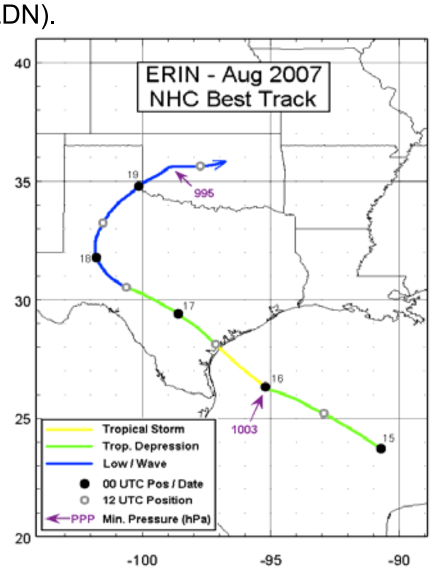


*Fig. 1: National Hurricane Center's best track of TC Erin, August 2007. Shaded circles indicate the system's location at 00 UTC and open circles indicate the location at 12 UTC, for the given day. Minimum pressure (hPa) over water and land are indicated by the purple arrows. Image adapted from Monteverdi et al. (2010).*

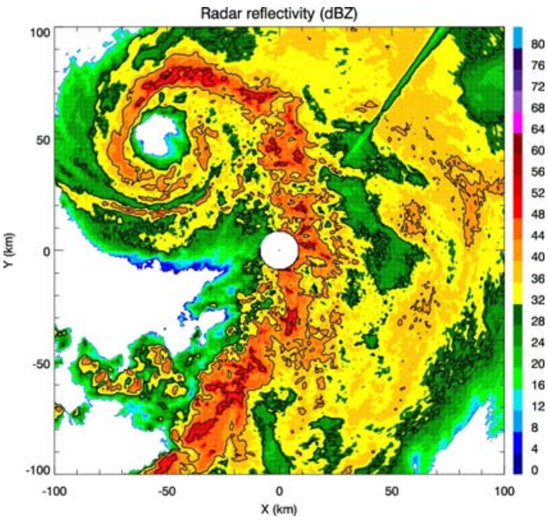


*Fig. 2: CAPPI of $Z_H$ at 3 km illustrating the distinct eye-like feature at 1013 UTC 19 August 2007. $Z_H$ is contoured at 30, 40, and 50 dBZ.*

## 2. BACKGROUND

Five other Tropical Cyclones (TCs) have reached OK while retaining tropical storm-force winds, although they differed from Erin in that they were in a dissipating stage rather than a re-intensifying stage at the time (Arndt et al. 2009). The re-intensification of Erin was atypical since it occurred well inland, about 800 km from the location of its landfall, and attained stronger sustained winds (25 m $s^{-1}$ with isolated gusts as high as 37 m $s^{-1}$) and a lower central pressure (995 hPa) than while over water (18 m $s^{-1}$ and 1003 hPa, respectively; Knabb 2008, Arndt et al. 2009). . While the overland re-intensification of Erin was undoubtedly a rare event, similar cases have been documented (Bosart and Lackmann 1995, Emanuel et al. 2008). Furthermore, studies such as Bassil and Morgan (2005) and Emanuel et al. (2008) have suggested that favorable surface conditions, such as warm and moist soils, may contribute to overland re-intensification.

Although the system produced strong surface winds and heavy rainfall over OK, the National Hurricane Center did not re-classify it as a tropical storm due to its transient lifespan; rather they concluded Erin was a “low.” Observations of the radar data, however, reveal several similarities to those documented for TCs over open water. For example, the eyewall convection of Erin during the period of re-intensification is noted to slope outward with height, which is one of the main characteristics of an eyewall within a mature TC (Houze 2010). Furthermore, a region of intense convection (hereafter termed a convective event (CE)) that formed within the eyewall during the re-intensification process appears to be similar to the “convective bursts” that have been related to TC intensification over water (Houze 2010). This CE appeared to go through a growth and decay process as it rotated around the eyewall between approximately 0803 UTC through 1003 UTC. It is presented in order to examine the structure of the deep convective updrafts (as indicated by columns of high $Z_{DR}$) and downdrafts. During this period, the center of Erin’s eye was located as far as 94 km and as close as 77 km from the KOUN radar. The CE was co-located with a cluster of enhanced lightning activity, evident in the OKLMA and NLDN data.

Recent observational studies have shown that lightning bursts within hurricane eyewalls may be related to TC intensification. Some studies have suggested eyewall lightning bursts may be a precursor to intensification (Black et al. 1993, Molinari et al. 1994, Price et al. 2009, Lyons et al. 1989), while others have observed them to occur either at the beginning of or during the time of intensification (Molinari et al. 1994, 1999, Fierro et al. 2007, 2011a, 2011b, Squires and Businger 2008). Demaria and Demaria 2009 have suggested that lightning bursts at larger radii, outside of the eyewall, may be better correlated with TC intensification.

## 3. INSTRUMENTATION AND DATA PROCESSING

Instrumentation used in this study include the polarimetric NOAA/National Severe Storms Laboratory KOUN WSR-88D radar, the Oklahoma Lightning Mapping Array (OK-LMA), and the National Lightning Detection Network (NLDN). In addition to collecting conventional radar variables such as reflectivity ($Z_H$) and radial velocity ($V_r$), the polarimetric KOUN radar collects differential reflectivity ($Z_{DR}$), cross-correlation coefficient ($\rho_{hv}$), and differential phase ($\Phi_{DP}$).. To ensure optimal quality, the radar data were processed according to the procedures detailed by Ryzhkov et al. (2005). $Z_H$ and $Z_{DR}$ were corrected for attenuation and differential attenuation, $Z_{DR}$ and $\rho_{hv}$ were corrected for noise biases, and $\Phi_{DP}$ was unfolded, smoothed, and used to compute $K_{DP}$. After processing, the data were then interpolated to a three-dimensional (3D)-Cartesian grid with horizontal and vertical spatial resolutions of 0.5 km and a temporal resolution of 5 minutes, which approximately corresponded to the time interval needed to collect each radar resolution volume. The 3D grids were then used to generate constant altitude plan position indicator (CAPPI) and range height indicator (RHI) images of $Z_H$, $Z_{DR}$, and $\rho_{hv}$.

In this study, the OK-LMA is used to examine total lightning data. During the observation period, the OK-LMA consisted of a network of 10 ground-based measurement stations located in central OK. This array of sensors measures the electromagnetic radiation emitted by lightning as it propagates through the atmosphere. The signals are detected using an available very high frequency (VHF) television band (usually 60-66 MHz, Channel 3; Thomas et al. 2004). LMA sensors can detect one pulse approximately every 80-100 μs and therefore as many as 10,000 radiation sources each second (Krehbiel et al. 2002). A lightning flash may produce hundreds to thousands of VHF sources. The time and 3D location of radiation sources are determined by performing a least squares fit of measured differences in the time-of-arrival of signals received at six or more receiving stations, synchronized with Global Positioning System time (Rison et al. 1999). For this study, we limited goodness-of-fit values ($\chi^2$) to ≤ 2 and set a requirement of at least seven receivers to increase degrees of redundancy. This resulted in a reduction of the number of local sources unrelated to lightning discharge. According to Rison et al. (1999), lightning mapping array timing uncertainties over the network are 40-50 ns, which lead to horizontal and vertical location errors of approximately 50 m and 100 m, respectively. This investigation focuses on data within the 3D observational domain of the OK-LMA network, which is illustrated in Fig. 3.

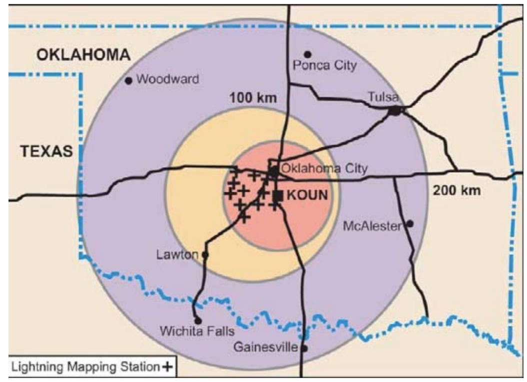


*Fig. 3: Map of Erin's observational domain. OK-LMA VHF receivers are indicated by cross symbols (+) and the location of KOUN is represented by a black square. The pink-shaded circle represents the area of optimum KOUN resolution (60 km radius). The gold-shaded circle (100 km radius) delimits the area in which 3D source locations are most accurately mapped. The purple-shaded region (200 km radius) delimits the area in which two-dimensional (2D) data are mapped well. Image adapted from MacGorman et al. (2008).*

For the data presented in this study, the OK-LMA's 3D observational domain completely overlaps the region of optimal KOUN data, allowing for a unique examination of the polarimetric and electrical characteristics of Erin's re-intensification. After the time and 3D locations of the VHF sources are measured, the total lightning activity can be mapped. The mapped data is not only useful for examining the electrical properties of storms, but also for determining their structure and intensity (Krehbiel et al. 2000). For further information on the specifications and accuracy of lightning mapping arrays, see Thomas et al. (2004). As a supplement to the OK-LMA, the NLDN provided the time, location, peak current, and polarity of ground-flash data.

## 4. OBSERVATIONAL ANALYSIS

Here we present Erin's polarimetric and electrical characteristics for the period during which the eye-like signature became most prominent in the radar imagery (0803-1258 UTC 19 Aug 2007). By 1258 UTC, the feature had begun to dissipate and exit the observational domain.

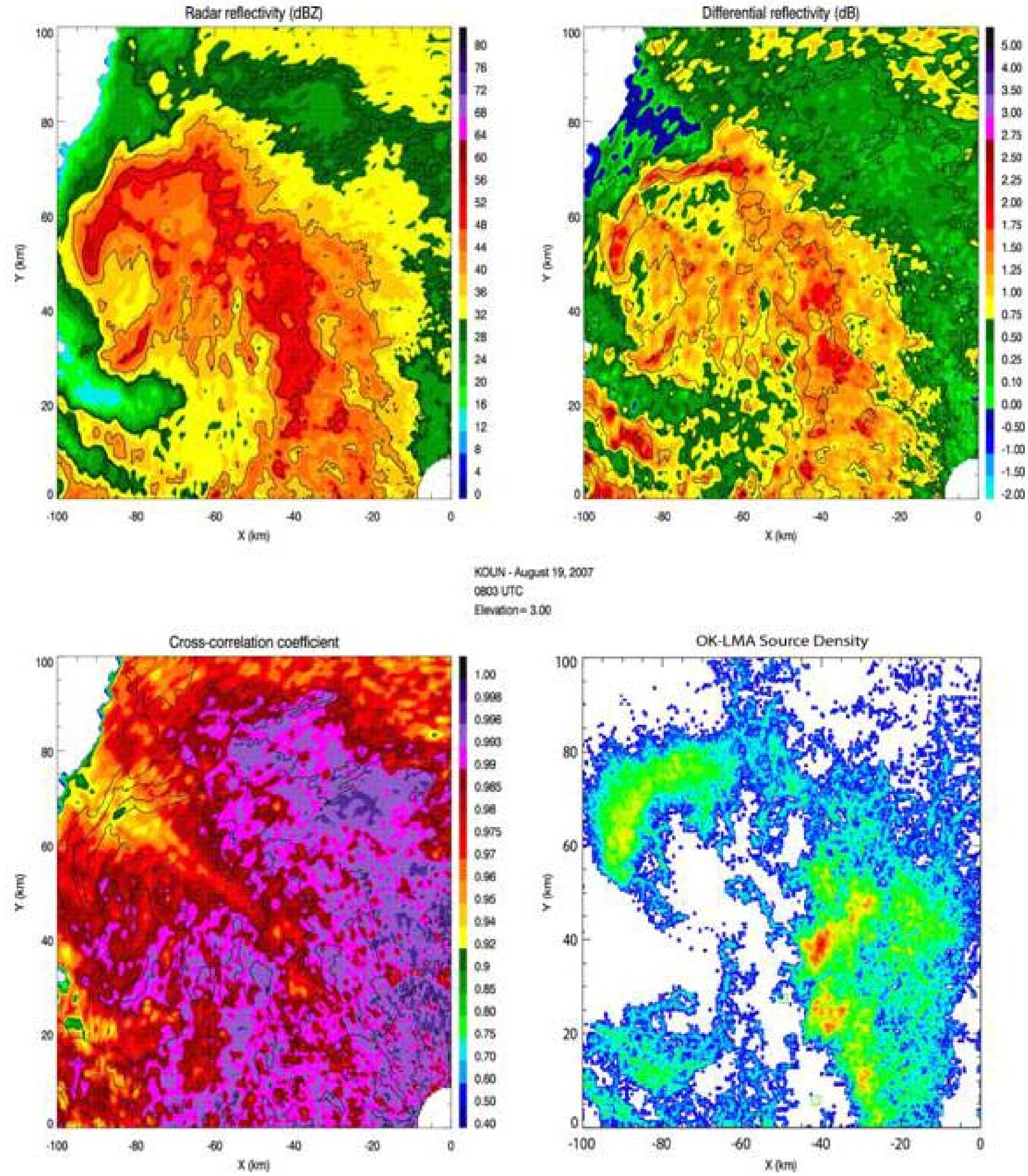


*Fig. 4: CAPPIs of $Z_H$, $Z_{DR}$, and $\rho_{hv}$ (top left/right, bottom left, respectively) at 3 km and OK-LMA total lightning source density (bottom right; 0803 UTC 19 August 2007). In each CAPPI, $Z_H$ is contoured at 30, 40, and 50 dBZ. Highest source densities are represented by red colors, and lowest source densities are represented by blue colors.*

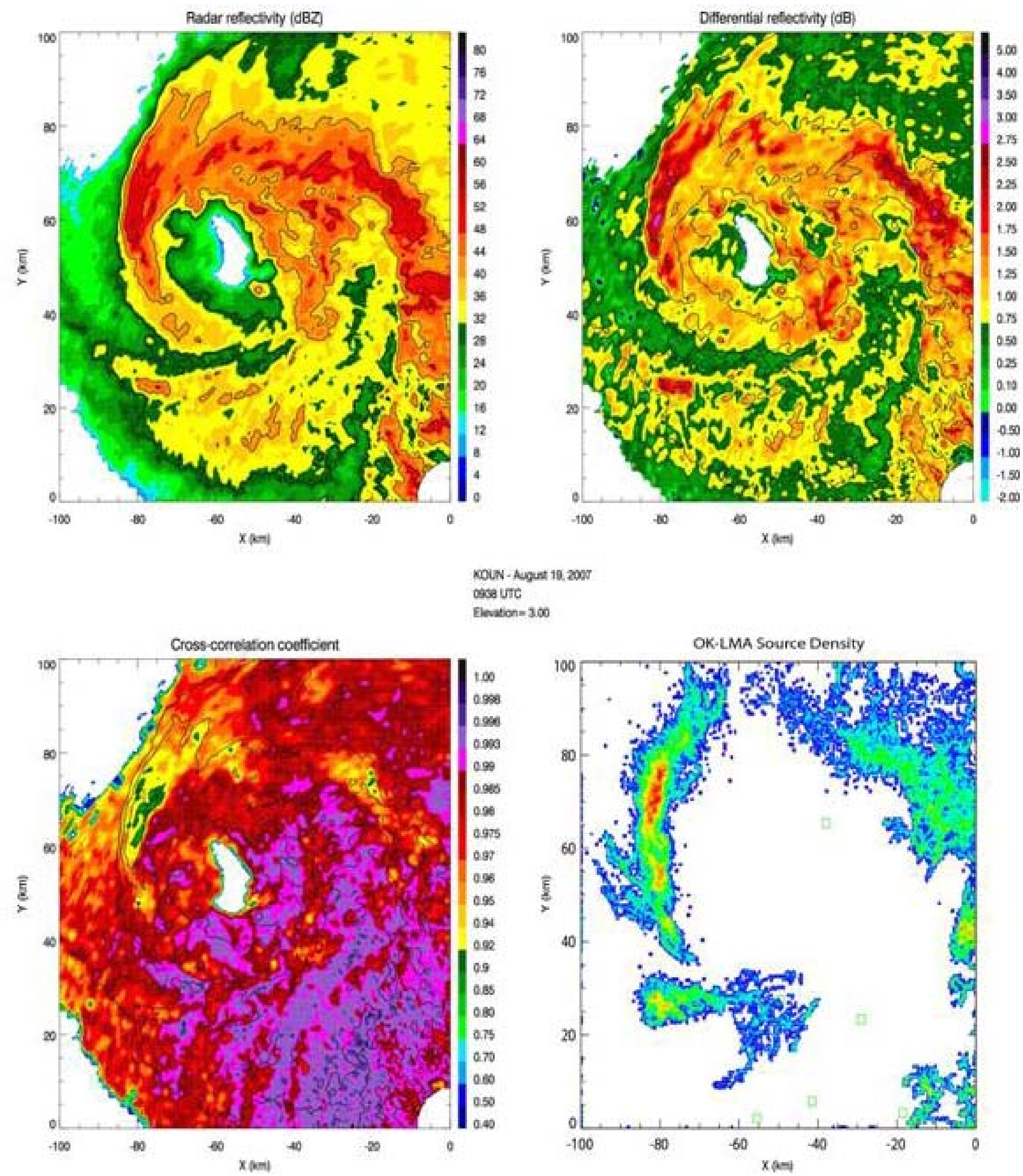


*Fig. 5: Same as Figure 4, except at 0938 UTC, 19 August 2007.*

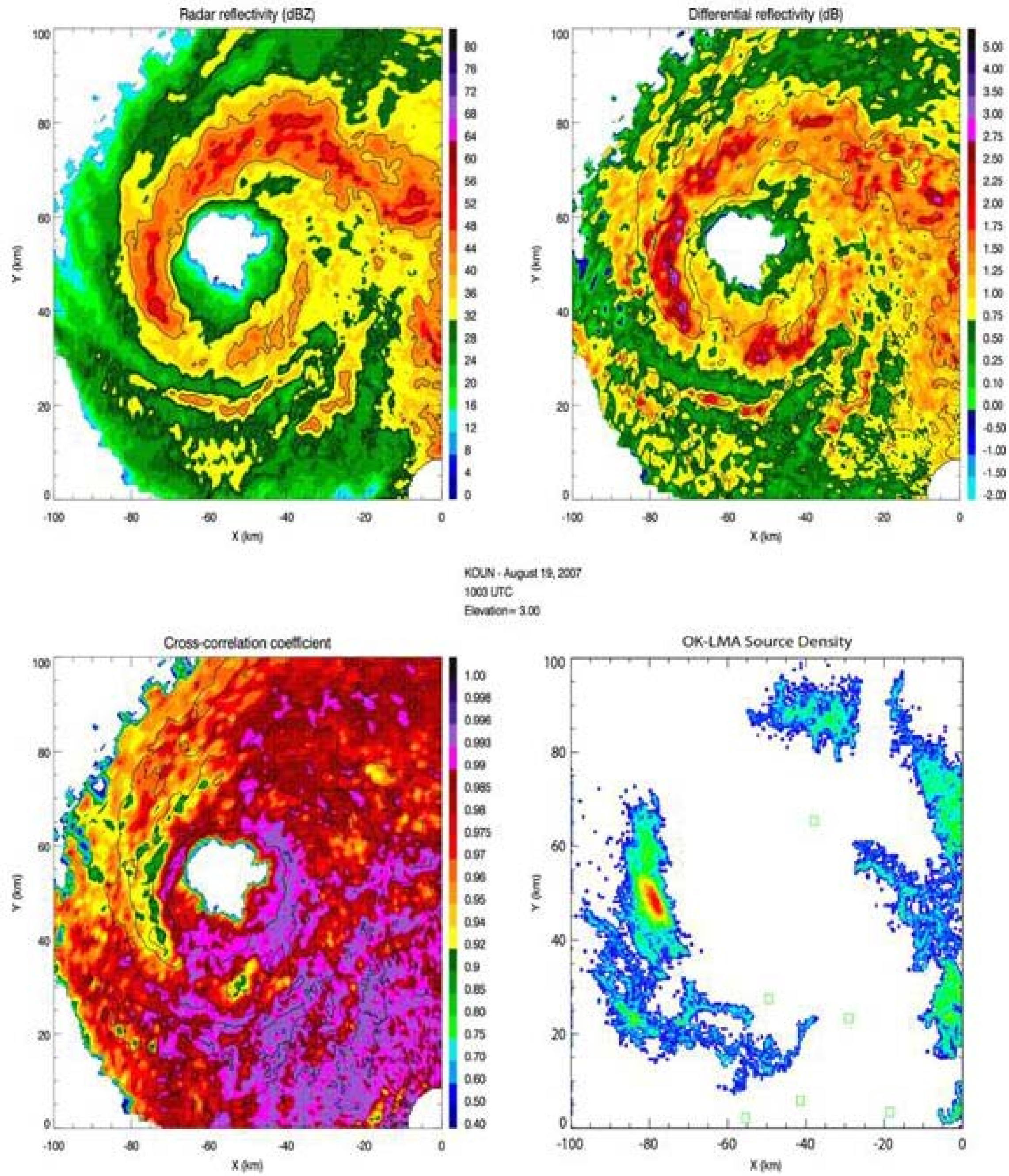


*Fig. 6: Same as Figure 4, except at 1003 UTC, 19 August 2007.*

### 4.1. *Eyewall Region*

*a) Convective event*

At 0803 UTC 19 August 2007, Erin had yet to exhibit an organized eyewall, but the center of circulation (approximately 94 km from KOUN) was re-strengthening as it progressed east-northeastward over central OK. Figure 4 presents the polarimetric variables and VHF source densities for the system at this time. A region of relatively intense convection within the northwest quadrant of the eyewall ($Z_H$ reaching 56-60 dBZ and $Z_{DR}$ reaching 2.25 dB) persisted in nearly the same location for approximately 1 hour, and then rotated cyclonically (Fig. 5) toward the southern quadrant of the eyewall, where it dissipated shortly after 1003 UTC

(Fig. 6). This CE appears to be similar to the convective bursts that have been related to TC intensification, and could therefore be related to Erin's overland re-intensification. Figures 5 and 6 display the polarimetric and VHF source densities for Erin at 0938 UTC and 1003 UTC, respectively, during the evolution of the CE. At 0938 UTC, the eyewall convection had become better organized with $Z_H$ and $Z_{DR}$ within the CE at 3 km reaching 60 dBZ and 3-3.5 dB, respectively. At 1003 UTC, the eye was distinct, with $Z_H$ as high as 56 dBZ and $Z_{DR}$ as high as 3-3.5 dB. Shortly after 1003 UTC, the CE dissipated. During the growth and decay process, the large $Z_{DR}$ values at the 3 km height level extended up to (and sometimes above) the freezing level (~ 4.5 km), as seen in several RHI images during the study, suggesting the presence of deep convective updrafts. Throughout its growth and decay period, NLDN (not shown) and OK-LMA data reveal that the CE was also co-located with a local maximum in total lightning activity. Compared with other regions of the eyewall during the observation period, this particular CE exhibited the largest VHF source densities.

*b) Sloping eyewall*

Figs. 7 and 8, at 0858 UTC, depict the eyewall structure along the 313° azimuth, which cuts through a portion of the main rainband and the northeast region of the eye. A well-defined melting layer is evident in the $\rho_{hv}$ signature ($\rho_{hv}$ < 0.95) at approximately 4.5 km. The layer appears elevated at the locations of convective towers, including in the eyewall convection. The $Z_H$ and $V_r$ signatures also both reveal organized eyewall convection that clearly slopes outward from the center of the eye with height. This feature has a very similar appearance to that of eyewall convection found within mature TCs. Another interesting feature in the polarimetric data is the relative lack of columns of high $Z_{DR}$ extending well above 0°C level. This is interesting since continental convection typically consists of an abundance of $Z_{DR}$ columns in locations where $Z_H$ values are enhanced. On another note, although the $Z_H$ values within the center of the eye are 20-36 dBZ in this image, values of near 0 dBZ have been observed at different times and azimuths. The sloping eyewall, a lack of $Z_{DR}$ columns, strong rising motion within the eyewall region (as suggested by the strong, low-level convergence), and reflectivities near 0 dBZ within the eye all indicate that Erin was exhibiting tropical-cyclone-like characteristics over central OK.

### 4.2. *Rainband Region*

*a) Tropical precipitation*

Figs. 9 and 10, at 1013 UTC, illustrate an area of heavy precipitation located along the 335° azimuth within the northern-most region of Erin's main rainband, northeast of the center of circulation. At a range of approximately 80 km, this precipitation exhibited moderate $Z_H$ values (up to 52 dBZ) and low $Z_{DR}$ values (mainly below 2 dB), indicating heavy rainfall dominated by small precipitation drops. This further signifies Erin's maritime tropical characteristics. Additionally, the $\rho_{hv}$ signature displays an absence of the melting layer within the heavy rainfall region ($\rho_{hv}$ mainly > 0.97). The $\rho_{hv}$ values suggest relatively small hydrometeor diversity, with perhaps some mixture of graupel within the rain.

*b) $Z_{DR}$ column*

Figs. 11 and 12, at 0838 UTC, display the location and signature of a particular area of strong convection within the main rainband. Along an azimuth of 321°, a convective tower is located at a range of 55-60 km, where $Z_H$ values of mainly 56-60 dBZ extend above 7.5 km. The tower is also characterized by a $Z_{DR}$ column that extends above the freezing layer to approximately 6.5 km in height, with $Z_{DR}$ values throughout the column reaching 2.25 dB. Additionally, while $\rho_{hv}$ values were generally greater than 0.97, a pocket of values as low as 0.85 was located at the top of and just above the convection. The column of high $Z_H$ and $Z_{DR}$, along with the local minimum in $\rho_{hv}$ atop the tower, suggests large precipitation particles were being elevated by a strong updraft. Furthermore, the reduction in $\rho_{hv}$ values atop the tower suggests drops were being lofted well above the freezing layer, as high as 8 km. This type of event occurred more frequently within Erin's rainbands than within the eyewall convection, where $Z_{DR}$ columns were either non-existent or rarely extended above the freezing layer.

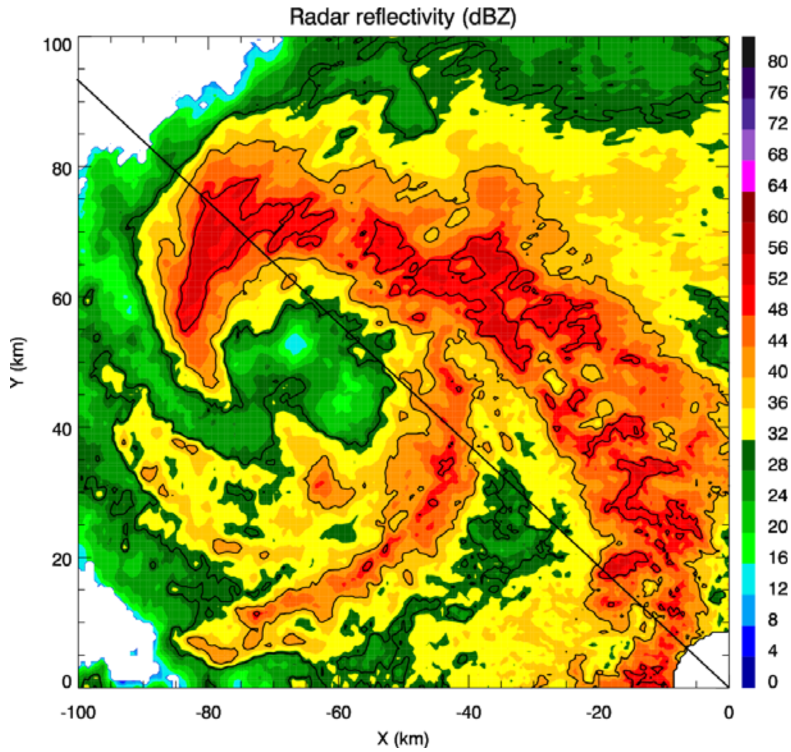


*Fig. 7: CAPPI of $Z_H$ at 3 km, for 0858 UTC, 19 August 2007. The black line indicates the location of the RHI in Fig. 8. $Z_H$ is contoured at 30, 40, and 50 dBZ.*

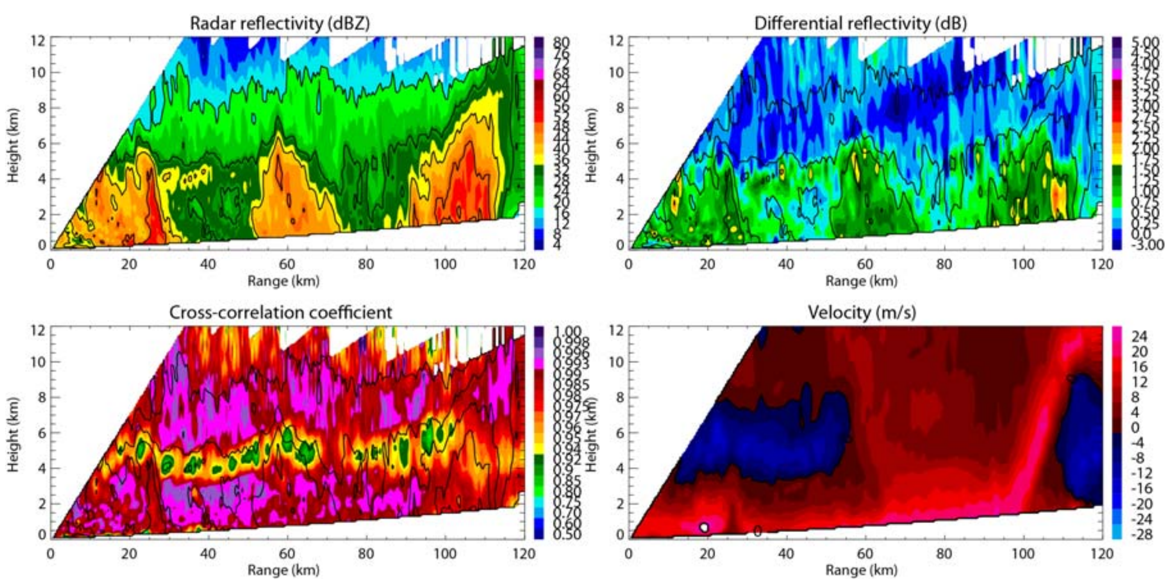


*Fig. 8: RHIs of $Z_H$, $Z_{DR}$, $\rho_{hv}$, and $V_r$ (top left/right, bottom left/right respectively) at 313° azimuth for 0858 UTC, 19 August 2007. In each RHI, $Z_H$ is contoured at 20, 30, 40, and 50 dBZ.*

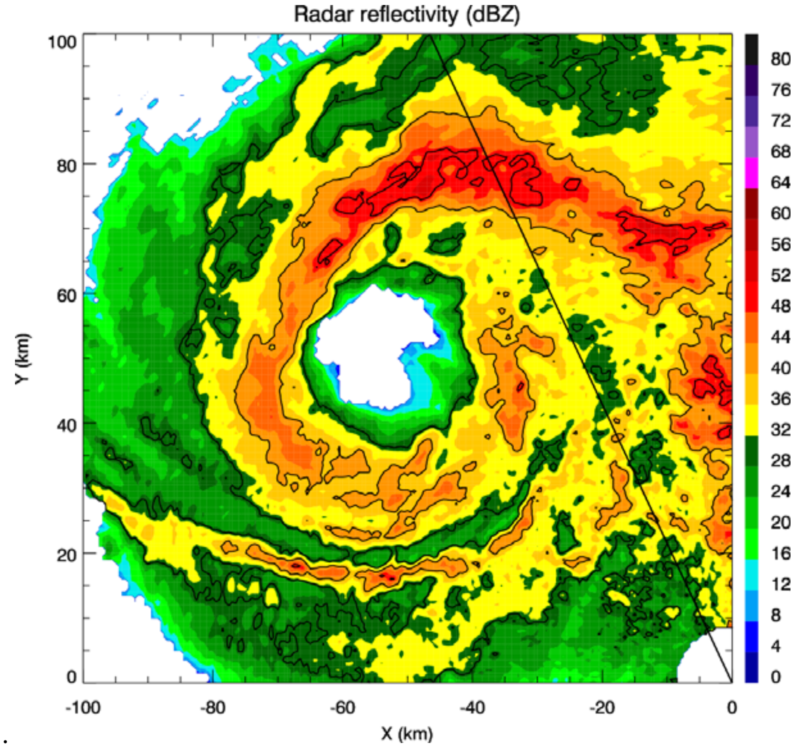


Fig. 9: CAPPI of $Z_H$ at 3 km, for 1013 UTC, 19 August 2007. The black line indicates the location of the RHI in Fig. 10. $Z_H$ is contoured at 30, 40, and 50 dBZ.

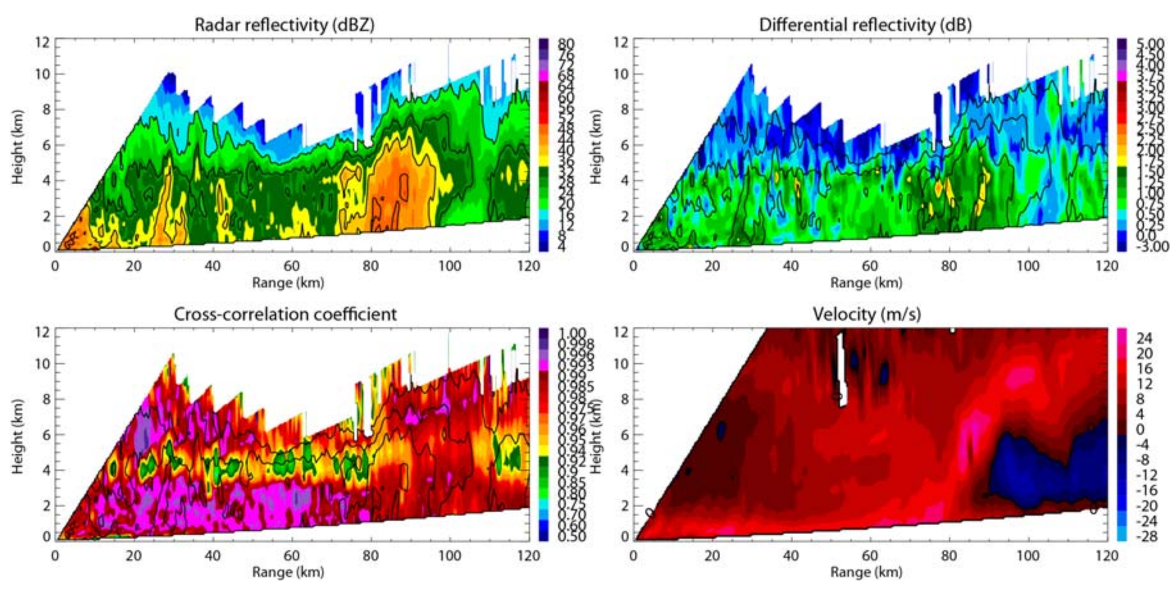


Fig. 10: RHIs of $Z_H$, $Z_{DR}$, $\rho_{hv}$, and $V_r$ (top left/right, bottom left/right respectively) at 335° azimuth for 1013 UTC, 19 August 2007. In each RHI, $Z_H$ is contoured at 20, 30, 40, and 50 dBZ.

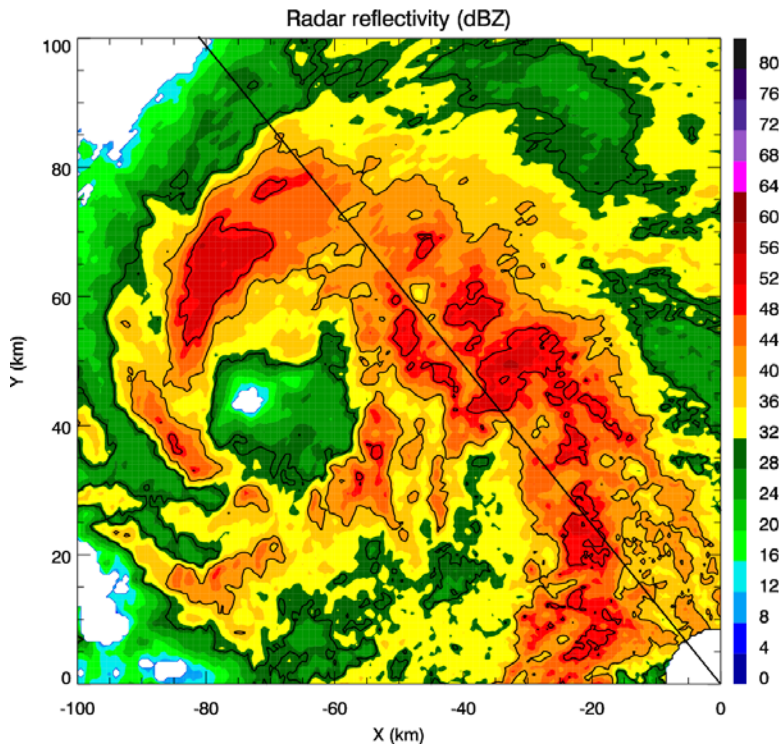


*Fig. 11: CAPPI of $Z_H$ at 3 km for 0838 UTC, 19 August 2007. The black line indicates the location of the RHI in Fig. 12. $Z_H$ is contoured at 30, 40, and 50 dBZ.*

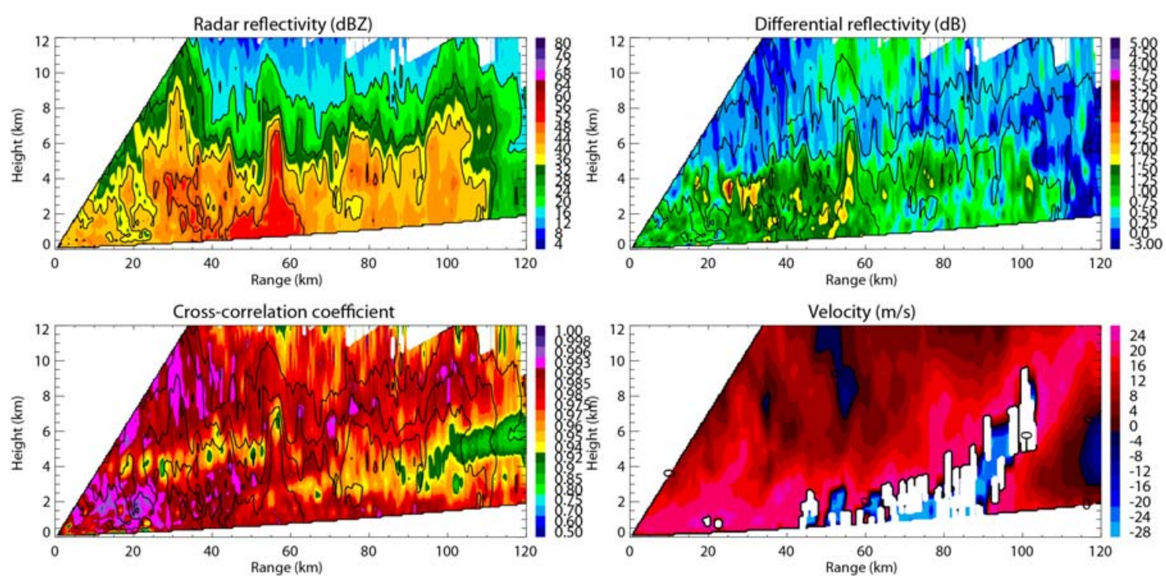


*Fig. 12: RHIs of $Z_H$, $Z_{DR}$, $\rho_{hv}$, and $V_r$ (top left/right, bottom left/right respectively) at 321° azimuth for 0838 UTC, 19 August 2007. In each RHI, $Z_H$ is contoured at 20, 30, 40, and 50 dBZ.*

### 4.3. *Stratiform Region*

*a) Depolarization Streaks*

Figures 13 and 14 (0803 UTC) are presented to illustrate the distinct signature of a depolarization streak located within Erin's leading stratiform precipitation region. At an azimuth of 350°, a radial streak of enhanced $Z_{DR}$ values extends from a range of approximately 60 km and a height of approximately 6.5 km. $Z_{DR}$ values are primarily larger than 2.25 dB, with maximum values reaching 3.50 dB. According to Ryzhkov et al. (2007), this enhancement of the $Z_{DR}$ field is due to canting of ice crystals within the strong electrostatic field aloft. Another significant feature in Fig. 14 is the $V_r$ signature. Near the surface, strong inbound velocities exceed 24 m $s^{-1}$, meeting tropical storm force wind classification.

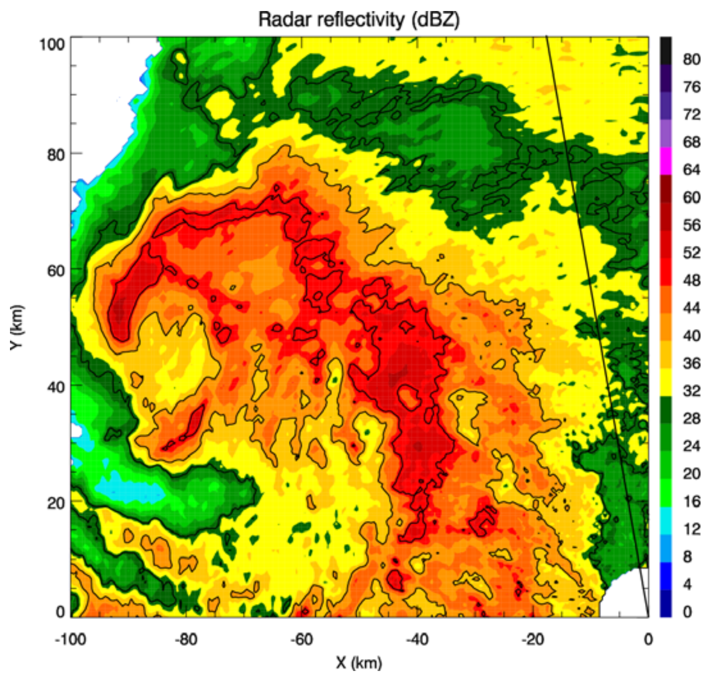


*Fig. 13: CAPPI of $Z_H$ at 3 km for 0803 UTC, 19 August 2007. The black line indicates the location of the RHI in Figure 14. $Z_H$ is contoured at 30, 40, and 50 dBZ.*

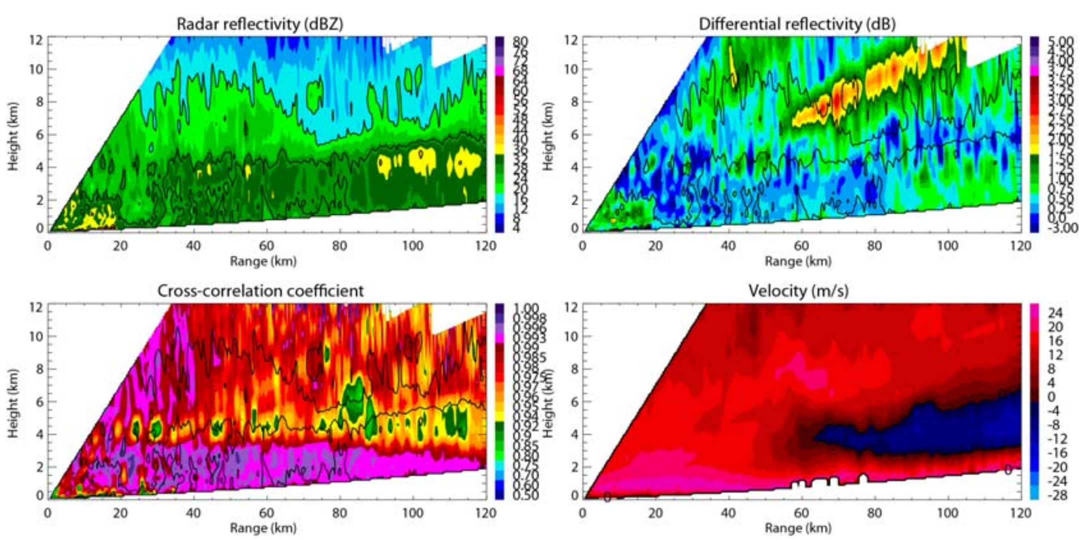


*Fig. 14: RHIs of $Z_H$, ZDR, $\rho_{hv}$, and $v_r$ (top left/right, bottom left/right respectively) at 350° azimuth for 0803 UTC, 19 August 2007. In each RHI, $Z_H$ is contoured at 20, 30, 40, and 50 dBZ.*

## 5. CONCLUSIONS

The overland re-intensification of TC Erin was an extraordinary event. While traversing OK on 19 August 2007, the system exhibited several characteristics similar to those that have been observed in tropical systems over water. This study examined the polarimetric structure of the eyewall and rainband convection during the re-intensification period, in an effort to compare Erin's convection to that of tropical systems that have been observed over water, as well as to gain a better understanding of the potential role the eyewall convection may have played in the re-intensification process. Lightning data from the OK-LMA and NLDN were also presented to convey the electrical structure of a region of intense eyewall convection that appeared to be similar to the convective bursts that have been related to tropical storm intensification over water. A region of maximum total lightning activity was correlated and dissipated with this CE throughout its lifetime. This is a particularly interesting attribute, since recent observational studies have shown that lightning bursts within hurricane eyewalls may be related to TC intensification. Other observed features that exemplified Erin's tropical nature include eyewall convection that sloped outward with height (with strong vertical velocities within the inner eyewall region), and heavy rainfall dominated by small precipitation drops. Furthermore, there was an overall lack of $Z_{DR}$ columns in locations of enhanced $Z_H$ values, dissimilar to what is typically observed in continental convection. This study also presented observations of a strong convective tower located within the main rainband, which consisted of a column of large $Z_H$ and $Z_{DR}$ values that extended well above the freezing layer. A pocket of low $\rho_{hv}$ values atop the tower suggests drops were being lofted as high as 8 km, something that was rarely observed to occur within the eyewall convection. Lastly, a distinct depolarization signature within the $Z_{DR}$ field demonstrated the presence of a strong electrostatic field aloft.

In future investigations, we will build upon this study to obtain a stronger understanding of Erin's re-intensification process. Research goals include analysis of the evolution of positive versus negative cloud-to-ground lightning flashes that occurred within a 40-50 km radius from the center of the eye, and differences in electrical characteristics between eyewall and rainband total lightning. Additionally, the authors will examine a period when total lightning within the eyewall rapidly ceased, despite the system retaining the eyelike feature in radar imagery.

## 6. ACKNOWLEDGEMENTS

The authors would like to acknowledge support for this work from the National Science Foundation Grant ATM-0924621.

## 7. REFERENCES

Arndt, D. S., J. B. Basara, R. A. McPherson, B. G. Illston, G. D. McManus, and D. B. Demko, 2009: Observations of the overland reintensification of Tropical Storm Erin (2007). *Bull. Amer. Meteor. Soc.,* **90**, 1079-1093.

Bassil, N. P. and M. C. Morgan, 2006: The overland reintensification of Tropical Storm Danny (1997). Preprints, 27th Conf. on Hurricanes and Tropical Meteorology, Monterey, CA, Amer. Meteor. Soc., 6A.6. [Available online at http://ams.confex.com/ams/pdfpapers/108676.pdf.]

Black R. A., Hallett J., Saunders C.P.R. (1993): Aircraft studies of precipitation and electrification in hurricanes. Preprints, 17th Conf. on Severe Local Storms, St. Louis, Amer. Meteor. Soc., pp J20-J25.

Bosart, L. F. and G. M. Lackmann, 1995: Postlandfall tropical cyclone reintensification in a weakly baroclinic environment: a case study of Hurricane David (1979). *Mon. Wea. Rev.,* **123**, 3268-3291.

DeMaria, M., and R. T. DeMaria, 2009: Applications of lightning observations to tropical cyclone intensity forecasting. Preprints, *16th Conference on Satellite Meteorology and Oceanography,* Phoenix, AX, Amer. Meteor. Soc., 1.3. [Available online at http://ams.confex.com/ams/89annual/techprogram/paper_145745.htm.]

Emanuel, K. A., J. Callaghan, and P. Otto, 2008: A hypothesis for the re-development of warm-core cyclones over northern Australia. *Mon. Wea. Rev.,* **136**, 3863-3872.

Houze, R. A., 2010: Clouds in tropical cyclones. *Mon. Wea. Rev.,* **138**, 293-344.

Knabb, R. D., 2008: Tropical Storm Erin. National Hurricane Center, 17 pp. [Available online at www.nhc.noaa.gov/pdf/TCR-AL052007_Erin.pdf.]

Krehbiel, P. R., R. J. Thomas, W. Rison, T. Hamlin, J. Harlin, and M. Davis, 2000: Lightning mapping observations in central Oklahoma, *EOS Trans. AGU,* **81**, 21-25.

Krehbiel, P., T. Hamlin, Y. Zhang, J. Harlin, R. Thomas, W. Rison, 2002: Three-dimensional total lightning observations with the lightning mapping array. Preprints, *International Lightning Detection Conference*, Tuscon, AZ, 6 pp.

Lyons W. A., Venne M. G., Black P. G., Gentry R. C. (1989): Hurricane lightning: A new diagnostic tool for tropical storm forecasting? Preprints, 18th Conf. on Hurricanes and Tropical Meteorology, San Diego, Amer. Meteor. Soc., pp 113-114.

Price, C., M. Asfur, and Y. Yair, 2009: Maximum hurricane intensity preceded by increase in lightning frequency. *Nat. Geo-sci.,* **2,** 329-332, doi: 10.1038/NGEO477.

Fierro, A. O., L. M. Leslie, E. R. Mansell, J. M. Straka, D. R. MacGorman, and C. Ziegler, 2007: A high-resolution simulation of microphysics and electrification in an idealized hurricane-like vortex. *Meteor. Atmos. Phys.,* **98**, 13-33, doi:10.1007/s00703-006-0237-0.

Fierro, A. O., X.-M. Shao, J.M. Reisner, J. D. Harlin, and T. Hamlin, 2011a: Evolution of eyewall convective events as indicated by intra-cloud and cloud-to-ground lightning activity during the rapid intensification of Hurricanes Rita, Katrina, and Charley. *Mon. Wea. Rev.,* ***139**,* 1492-1504.

Fierro, A. O., and J. M. Reisner, 2011b: High-resolution simulation of the electrification and lightning of Hurricane Rita during the period of rapid intensification. *J. Atmos. Sci.,* **68**, 477-494.

MacGorman, D. R., W. D. Rust, T. J. Schuur, M. I. Biggerstaff, J. M. Straka, C. L. Ziegler, E. R. Mansell, E. C. Bruning, K. M. Kuhlman, N. R. Lund, N. S. Biermann, C. Payne, L. D. Carey, P. R. Krehbiel, W. Rison, K. B. Eack, and W. H. Beasley, 2008: TELEX: The Thunderstorm Electrification and Lightning Experiment. *Bull. Amer. Meteor. Soc*., **89**, 997-1013, DOI: 10.1175/2007BAMS2352.1.

Molinari J., Moore P. K., Idone V. P., Henderson R., Saljoughy A. B. (1994): Cloud-to-ground lightning in hurricane Andrew. *J. Geophys. Res. Atmos*. 99: 16665-676.

Molinari, J., P. Moore, and V. Idone, 1999: Convective structure of hurricanes as revealed by lightning locations. *Mon. Wea. Rev.,* **127**, 520-534.

Monteverdi, J. P., and R. Edwards, 2010: The redevelopment of a warm-core structure in Erin: a case of inland tropical storm formation. *Electronic J. Severe Storms Meteor.,* **5 (6)**, 1-18.

Rison, W., R. J. Thomas, P.R. Krehbiel, T. Hamlin, and J. Harlin, 1999: A GPS-based three-dimensional lightning mapping system: Initial observations in central New Mexico. *Geophys. Res. Lett.,* **26**, 3573-3576.

Ryzhkov, A. V., S. E. Giangrande, and T. J. Schuur, 2005: Rainfall estimation with a polarimetric prototype of WSR-88D. *J. Appl. Meteor.,* **44**, 502-515.

Ryzhkov, A. V., and D. S. Zrnić, 2007: Depolarization in ice crystals and its effect on radar polarimetric measurements. *J. Atmos. Oceanic Technol.,* **24**, 1256-1267.

Squires, K., and S. Businger, 2008: The morphology of eyewall lightning outbreaks in two category 5 hurricanes. *Mon. Wea. Rev.,* **136,** 1706-1726.

Thomas, R., P. Krehbiel, W. Rison, S. Hunyady, W. Winn, T. Hamlin, and J. Harlin, 2004: Accuracy of the lightning mapping array. *J. Geophys. Res.,* **109**, D14207, doi:10.1029/2004JD004549.